Critical number of walkers for diffusive search processes with resetting

Marco Biroli [1], Satya N. Majumdar [1] and Grégory Schehr [2]
[1] *LPTMS, CNRS, Univ. Paris-Sud, Université Paris-Saclay, 91405 Orsay, France*
[2] *Sorbonne Université, Laboratoire de Physique Théorique et Hautes Energies, CNRS UMR 7589, 4 Place Jussieu, 75252 Paris Cedex 05, France*

(Received 13 April 2023; accepted 30 May 2023; published 27 June 2023)

We consider N Brownian motions diffusing independently on a line, starting at $x_0 > 0$, in the presence of an absorbing target at the origin. The walkers undergo stochastic resetting under two protocols: (A) each walker resets *independently* to x_0 with rate r and (B) all walkers reset *simultaneously* to x_0 with rate r. We derive an explicit analytical expression for the mean first-passage time to the origin in terms of an integral which is evaluated numerically using *Mathematica*. We show that, as a function of r and for fixed x_0, it has a minimum at an optimal value $r^* > 0$ as long as $N < N_c$. Thus resetting is beneficial for the search for $N < N_c$. When $N > N_c$, the optimal value occurs at $r^* = 0$ indicating that resetting hinders search processes. We obtain different values of N_c for protocols A and B; indeed, for $N \leqslant 7$ resetting is beneficial in protocol A, while for $N \leqslant 6$ resetting is beneficial for protocol B. Our theoretical predictions are verified in numerical Langevin simulations.

DOI: 10.1103/PhysRevE.107.064141

I. INTRODUCTION

Search processes are ubiquitous in nature and human behavior [1–3] with examples ranging from foraging animals [4,5] to proteins trying to bind on DNA [6–9]. In most of these examples there is an interest in optimizing the search process, i.e., minimizing the time taken to reach the target by varying some underlying parameters of the dynamics. One preeminent family of efficient search processes is the so-called *intermittent* search strategies [10–12]. For these processes, the searcher or the agent alternates between short- and long-range steps. During the short-range steps the agent actively searches for the target. Instead, the long-range steps allow it to explore new areas of the space. Resetting search processes are examples of efficient intermittent search processes [13–16], where after a certain time, random or nonrandom, the agent gives up on its current path and restarts from some other place; for a recent review see [17].

While the idea of introducing resetting in a search process had been used empirically before, a quantitative computation of the search time was performed first in Refs. [18,19] in a simple model of a Brownian agent searching for a fixed target in space. For example, in the simplest case in one dimension, consider a fixed target at the origin and a Brownian searcher with diffusion constant D that starts at the initial position x_0 and resets to x_0 after an exponentially distributed random time with rate r. The target is found when the walker reaches the origin for the first time at $t = t_f$. Hence the mean search time is just the mean first-passage time (MFPT) $\langle t_f \rangle_r(x_0)$ to the origin, starting from x_0. One of the main findings of Ref. [18] was that while the MFPT diverges in the absence of resetting ($r = 0$), it is finite for $r > 0$ and is given by

$$\langle t_f \rangle_r(x_0) = \frac{1}{r}\,(e^{\sqrt{r/D}\,|x_0|} - 1). \tag{1}$$

For a fixed x_0, the MFPT in Eq. (1), as a function of r, has a unique minimum at $r = r^* = R^*\,x_0^2/D$, where the dimensionless optimal rate $R^* = 2.53962\ldots$ is easily found by minimizing Eq. (1) with respect to r and is given by the unique root of $\sqrt{R} - 2 + 2\,e^{-\sqrt{R}} = 0$. Thus, not only does the resetting render the MFPT finite, it can even be optimized by choosing the resetting rate to be r^*. Subsequently, numerous models of search processes with resetting found the existence of an optimal r^* [20–31]. For simple diffusion with resetting in one and two dimensions, the optimal r^* was measured recently in optical tweezer experiments [32–34].

One naturally wonders if resetting is always advantageous, i.e., whether the optimal r^* is strictly positive. This question has been addressed in several papers for general single-particle search process subject to resetting. It turns out that in many search processes, the optimal value of r^* may undergo a transition from a nonzero value (resetting is beneficial) to zero (resetting is detrimental), as one tunes some additional parameter through a critical value in the underlying search process [21,24,26,35–44]. A simple example concerns the diffusive search of a fixed target at the origin in one dimension as discussed above, but now the searcher, starting and resetting to x_0, is confined in a box $[-L, L]$ with reflecting boundary conditions [35]. As $L \to \infty$, the MFPT is given by Eq. (1) with a nonzero r^*. As L decreases, the value of r^* decreases, and for $L \leqslant L_c$, the optimal resetting rate becomes zero, i.e., $r^* = 0$ [35]. Treating r^* as an order parameter of this resetting phase transition, some models exhibit a first-order transition (where r^* drops abruptly to zero), but some others a continuous transition (with r^* vanishing continuously). In Ref. [40] a Landau-like theory was developed to study this resetting phase transition with r^* as the order parameter.

This issue of the existence of an optimal r^* has not been addressed so far, to the best of our knowledge, when the search for the target is conducted by a team of N searchers with stochastic resetting. The purpose of this paper is to study

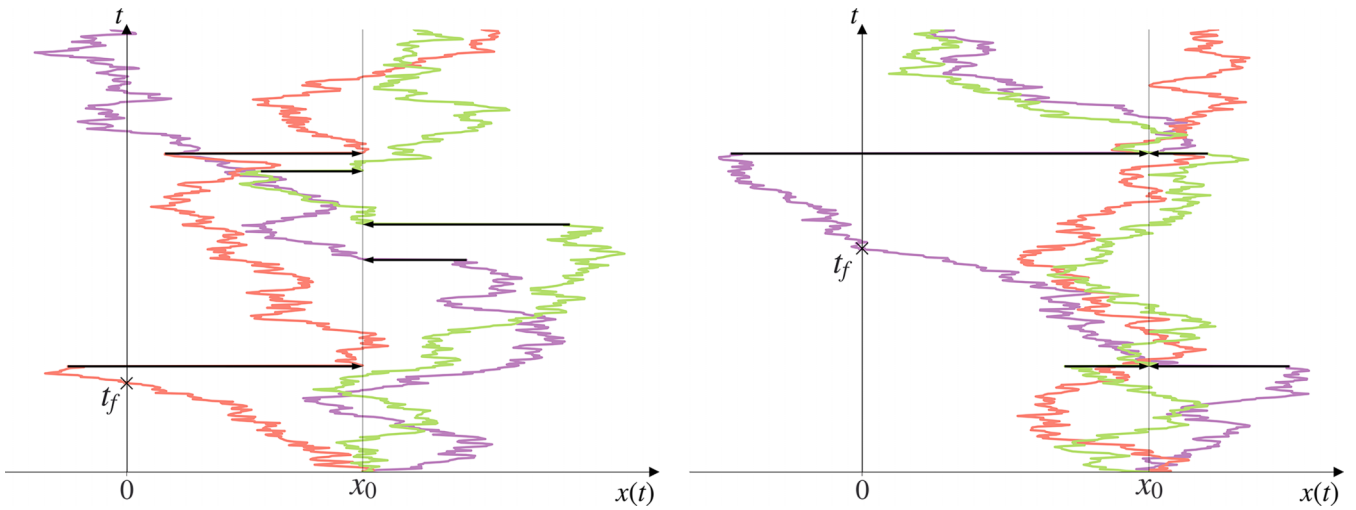

FIG. 1. Typical trajectories for $N = 3$ one-dimensional random walkers undergoing *independent* resetting (protocol A) in the left panel and *simultaneous* resetting (protocol B) in the right panel. Different colors correspond to different walkers, and the resetting events are shown with full black arrows. All the walkers start at $x_0 > 0$ and reset to x_0, and t_f denotes the first-passage time of the walkers to the target located at the origin $x = 0$.

the optimal r^* as a function of N in a simple model of N diffusive searchers on a line undergoing stochastic resetting at a constant rate r. To be precise, we will consider N diffusing particles on a line each with diffusion constant D and starting at the same initial position x_0, with the target fixed at the origin. Since the search process is symmetric with respect to the sign of x_0, we consider only $x_0 > 0$ without any loss of generality. For resetting, we will follow two distinct protocols:

1. *Protocol A.* In this protocol, each one of the N particles diffuses and resets to x_0 *independently* with rate r [18]. The positions of the particles are thus *uncorrelated* at all times. For a typical schematic representation of the trajectories see Fig. 1.

2. *Protocol B.* Here each one of the N particles diffuses independently, but they all reset *simultaneously* to x_0 with rate r [45]. This simultaneous resetting makes the particle positions *correlated* at all times t. See Fig. 1 for typical trajectories under the protocol B.

For $N = 1$, the two protocols coincide, but they are different for $N > 1$. In protocol A, the particles remain noninteracting at all times. This protocol was first studied in Ref. [18] with the initial positions of the searchers distributed uniformly with density ρ (i.e., $N \to \infty$ limit) on one side of the target at the origin and the authors computed exactly the Laplace transform of the survival probability of the target up to time t. From this Laplace transform, the exact asymptotic behavior of the survival probability at late times was extracted. In a recent work [46], the two-time correlation function of the maximum displacement of the N particles (without a target) was studied numerically. However, the MFPT to a target for fixed $N > 1$ has not been studied. Protocol B was recently introduced in Ref. [45], and it was shown that in the absence of a target, the system approaches at long times a many-body nonequilibrium stationary state with strong correlations between the positions of the particles. The stationary joint distribution of the positions of the particles was computed exactly. Despite strong correlations between particles, several observables such as the distribution of the position of the kth rightmost particle, the distribution of the successive gaps between particles, and so on were computed analytically in the stationary state in the limit of large N [45]. However, the MFPT to a target for finite $N > 1$ has not been computed for protocol B either.

In this paper we compute analytically the MFPT to the target by N Brownian searchers for both resetting protocols A and B defined above. For the optimal reset rate r^*, we find a rather interesting and somewhat surprising result for both protocols. We show that the MFPT, as a function of the reset rate r, exhibits a unique minimum at $r = r^*$. However, the optimal value r^* is strictly positive, i.e., the resetting is beneficial only for $N \leqslant 7$ in protocol A and $N \leqslant 6$ in protocol B. When $N \geqslant 8$ in protocol A or $N \geqslant 7$ in protocol B, the optimal resetting rate becomes $r^* = 0$. In those cases the MFPT is a monotonically increasing function of r with a minimum at $r = 0$, implying that resetting will only increase the mean search time and hence is detrimental to the search process. To understand the origin of these two magic numbers $N = 7$ and $N = 6$ in the two protocols, it is convenient to continue analytically our general formula for integer N to real N. Following the analytic continuation, we show that the actual transitions take place respectively at $N_c = 7.3264773\ldots$ (for protocol A) and $N_c = 6.3555864\ldots$ (for protocol B), which turn out to be the unique roots of two different transcendental equations.

The rest of the paper is organized as follows. In Sec. II we briefly recall how to compute the MFPT from the survival probability. In Sec. III and Sec. IV we present the exact computations of the MFPT, respectively, in protocol A and protocol B. We conclude in Sec. V and some details of the computations are presented in the Appendixes.

II. MEAN FIRST-PASSAGE TIME

We consider N Brownian particles that start at $x_0 > 0$ at $t = 0$ and undergo stochastic resetting with rate r following either protocol A or B defined above. We consider a stationary

target at the origin. Whenever any of the N walkers reach the origin, the search is terminated. We denote by t_f the first-passage time to the origin by this N-particle process (see Fig. 1). Clearly t_f is a random variable, and we will denote the MFPT by $\langle t_f \rangle_{r,N}^{(A)}(x_0)$ for protocol A and $\langle t_f \rangle_{r,N}^{(B)}(x_0)$ for protocol B. In order to compute $\langle t_f \rangle_{r,N}^{(A/B)}(x_0)$ it is useful to consider the cumulative distribution of t_f,

$$S_{r,N}^{(A/B)}(x_0, t) = \text{Prob.}\,[t_f \geqslant t], \tag{2}$$

known as the survival probability, i.e., the probability that none of the walkers have reached the target up to time t. Using Eq. (2), the MFPT can then be expressed quite generally for any process as [47–49]

$$\begin{aligned}\langle t_f \rangle_{r,N}^{(A/B)}(x_0) &= \int_0^{+\infty} t \left(-\frac{\partial S_{r,N}^{(A,B)}(x_0, t)}{\partial t} \right) dt \\ &= \int_0^{+\infty} S_{r,N}^{(A/B)}(x_0, t)\, dt, \end{aligned} \tag{3}$$

where, in the second equality, we used integration by parts and assumed that $t\, S_{r,N}^{(A/B)}(x_0, t) \to 0$ when $t \to +\infty$, which can be verified *a posteriori*. Hence to compute the MFPT we need to compute the survival probability $S_{r,N}^{(A/B)}(x_0, t)$. We will now treat protocols A and B separately.

III. PROTOCOL A

In protocol A we have N independent copies of a one-dimensional resetting random walker (see the left panel of Fig. 1). These walkers are independent at all times t. Hence

$$S_{r,N}^{(A)}(x_0, t) = [Q_r(x_0, t)]^N, \tag{4}$$

where $Q_r(x_0, t)$ is the survival probability of a single walker in the presence of resetting, starting at $x_0 > 0$ at $t = 0$. This survival probability for a single resetting walker has been extensively studied [18,19]. Let us briefly recall the derivation here for the sake of completeness.

For a single walker, using a renewal approach, one can relate the resetting survival probability to the survival probability without resetting ($r = 0$), namely [17],

$$\begin{aligned} Q_r(x_0, t) = e^{-rt} Q_0(x_0, t) + r \int_0^t d\tau e^{-r\tau} Q_0(x_0, \tau) \\ \times Q_r(x_0, t - \tau). \end{aligned} \tag{5}$$

This equation can be understood as follows. The first term in Eq. (5) represents the probability of the event when there are no resettings in the interval $[0, t]$ and the particle survives up to t, starting at x_0. The probability of no resetting in $[0, t]$ is e^{-rt}, and it then gets multiplied by the probability $Q_0(x_0, t)$ that the particle survives without resetting up to t, leading to the first term in Eq. (5). In the complementary case when the walker resets at least once to x_0, let us denote by $t - \tau$ the time of the last resetting event before t. Then with probability $r\, d\tau$ the walker resets at $t - \tau$ and with probability $e^{-r\tau}$ the walker does not reset again in $[t - \tau,\ t]$. In the interval $[0, t - \tau]$ the survival probability is just $Q_r(x_0, t - \tau)$, while in $[t - \tau,\ t]$ the survival probability is $Q_0(x_0, \tau)$ since there is no resetting in $[t - \tau, t]$. Using the renewal property of the process we then take the product of all these probabilities and integrate over all $\tau \in [0, t]$, leading to the second term in Eq. (5).

The convolution structure of the renewal equation naturally calls for the use of Laplace transform with respect t defined as

$$\tilde{Q}_r(x_0, s) = \int_0^{\infty} Q_r(x_0, t)\, e^{-st}\, dt. \tag{6}$$

Taking the Laplace transform of Eq. (5) and simplifying yields the result [17]

$$\tilde{Q}_r(x_0, s) = \frac{\tilde{Q}_0(x_0, s + r)}{1 - r\, \tilde{Q}_0(x_0, s + r)}. \tag{7}$$

Furthermore, the survival probability of a standard one-dimensional Brownian motion without resetting is given by the well-known formula [47–49]

$$Q_0(x_0, t) = \text{erf}\left(\frac{x_0}{\sqrt{4Dt}} \right), \tag{8}$$

where $\text{erf}(z) = (2/\sqrt{\pi}) \int_0^z e^{-u^2}\, du$. Its Laplace transform is given by

$$\begin{aligned} \tilde{Q}_0(x_0, s) &= \int_0^{+\infty} e^{-st} \text{erf}\left(\frac{x_0}{\sqrt{4Dt}} \right) dt \\ &= \frac{1}{s}\left(1 - e^{-x_0 \sqrt{\frac{s}{D}}}\right). \end{aligned} \tag{9}$$

For simplicity, from now on, we rewrite all the variables in terms of their dimensionless counterparts, i.e.,

$$S = \frac{x_0^2}{D} s, \quad R = \frac{x_0^2}{D} r, \quad T = \frac{D}{x_0^2} t. \tag{10}$$

Inserting the result from Eq. (9) in Eq. (7) gives, in terms of dimensionless variables,

$$\tilde{Q}_r(x_0, s) = \frac{x_0^2}{D} \frac{1 - e^{-\sqrt{S+R}}}{[S + R\, e^{-\sqrt{S+R}}]}. \tag{11}$$

Inverting this Laplace transform formally one gets

$$Q_r(x_0, t) = \int_\Gamma \frac{dS}{2\pi i}\, e^{ST} \frac{1 - e^{-\sqrt{S+R}}}{S + R\, e^{-\sqrt{S+R}}} \equiv q(R, T), \tag{12}$$

where Γ denotes the Bromwich contour in the complex S plane. Plugging this result into Eq. (4) and then using Eq. (3) we get the dimensionless MFPT

$$\langle T_f \rangle^{(A)}(R, N) = \frac{D}{x_0^2} \langle t_f \rangle_{r,N}^{(A)}(x_0) = \int_0^{+\infty} [q(R, T)]^N\, dT. \tag{13}$$

We inverted the Laplace transform in Eq. (12) numerically and then evaluated the integral in Eq. (13). In the right panel of Fig. 2 we compare this theoretical prediction with numerical Langevin simulation results by plotting $\langle T_f \rangle^{(A)}(R, N)$ as a function of R, for different values of N. We find excellent agreement. Physically it is clear that as $R \to +\infty$ we expect the MFPT $\langle T_f \rangle^{(A)}(R, N)$ to diverge since the system constantly resets and thus never explores the space. This can be seen by noting that $q(R, T) \to 1$ as $R \to +\infty$ in Eq. (12), and hence the integral of the MFPT in Eq. (13) diverges. Let us now investigate the opposite limit $R \to 0$. If the MFPT decreases at small R, then it is likely that there is a certain $R^\star > 0$ where the curve becomes a global minimum, before

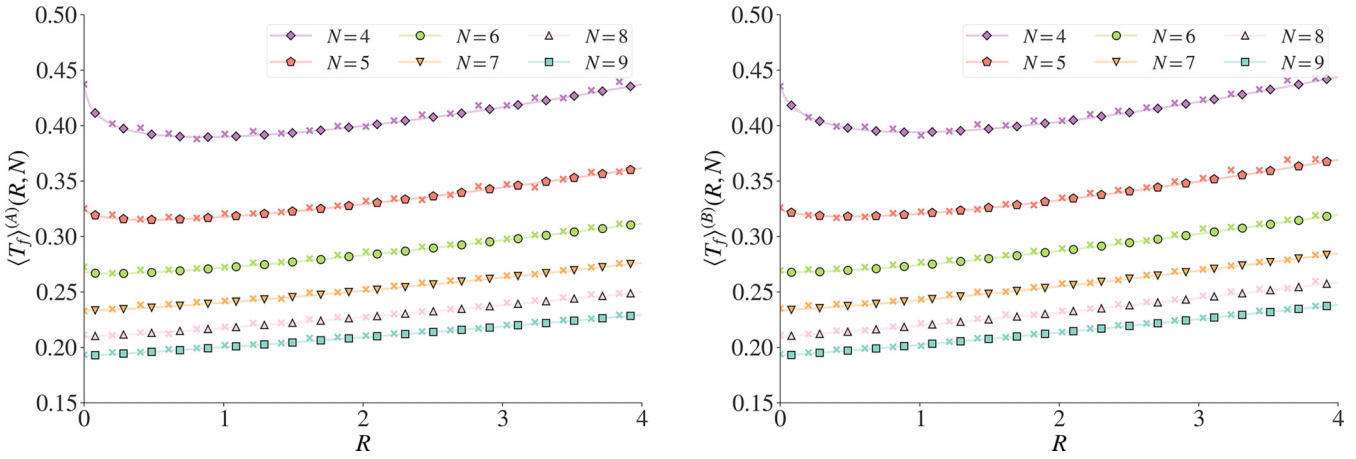

FIG. 2. Comparison of theoretical and numerical Langevin results for the mean first-passage time as a function of the resetting rate for protocol A (left panel) and protocol B (right panel). The solid lines with varying markers and colors correspond to the theoretical results given in Eq. (13) (left panel) and Eqs. (25) and (26) (right panel). The quantity $q(R,T)$ in Eq. (13) is computed by evaluating the Bromwich integral in Eq. (12) numerically. The crosses represent the results from numerical Langevin simulations with 10^5 samples. The different colors and markers correspond to different values of N, where N goes from 4 to 9 from top to bottom. Notice that in both panels we can observe the gradual disappearance of the minimum at $R^\star > 0$.

starting to increase again and finally diverging as $R \to \infty$ (see Fig. 2). However, if the MFPT increases for small R, then clearly $R^\star = 0$, provided the MFPT increases monotonically with increasing R as happens to be the case (see Fig. 2). Thus, the existence of a minimum $R^\star > 0$ can then be investigated by analyzing the small R behavior of $\langle T_f\rangle^{(A)}(R,N)$.

The small R asymptotic behavior of $\langle T_f\rangle^{(A)}(R,N)$ depends on the value of N. It can be analyzed using Eqs. (13) and (12), as shown in detail in Appendix A. In fact, even though the search process makes sense only for integer N, our analytical result in Eqs. (12) and (13) can be continued analytically to real N. Hence, from now on, we will consider N real in this sense. It turns out that if $N \leqslant 2$, then $\langle T_f\rangle^{(A)}(R,N)$ diverges as $R \to 0$, if $2 < N \leqslant 4$, then $\langle T_f\rangle^{(A)}(0,N)$ is finite but the slope of $\langle T_f\rangle^{(A)}(R,N)$ at $R \to 0$ is negatively divergent, and finally if $N > 4$, both the MFPT and its derivative are finite at $R = 0$. Let us summarize here the leading small R behavior of the MFPT for different values of N:

$$\langle T_f\rangle^{(A)}(R,N) \underset{R\to 0}{\sim} \begin{cases} \frac{\Gamma(1-N/2)}{\pi^{N/2}N^{1-N/2}}\frac{1}{R^{1-N/2}} & \text{if } N<2, \\ -\frac{1}{\pi}\ln R & \text{if } N=2, \\ C_N^{(A)} - \frac{2\,\Gamma(2-N/2)}{(N-2)\,\pi^{N/2}}\,N^{N/2-1}\,R^{N/2-1} & \text{if } 2<N<4, \\ C_N^{(A)} + \frac{4}{\pi^2}R\ln R & \text{if } N=4, \\ C_N^{(A)} + R\int_0^{+\infty}[q(0,T)]^{N-1}\frac{\partial q(R,T)}{\partial R}\Big|_{R=0}dT & \text{if } N>4, \end{cases} \tag{14}$$

where for any $N > 2$ the constant $C_N^{(A)}$ is given by

$$C_N^{(A)} = \langle T_f\rangle^{(A)}(0,N) = \int_0^{+\infty} \mathrm{erf}\left(\frac{1}{\sqrt{4T}}\right)^N dT. \tag{15}$$

For $N \leqslant 4$, the small R behavior of the MFPT above, combined with the divergence as $R \to \infty$, indicates the existence of a finite $R^\star > 0$ for all $N \leqslant 4$. However, for $N > 4$ one has to find the condition for a nonzero $R^\star > 0$. For $N > 4$ both the MFPT and its first derivative with respect to R are finite, and the sign of the derivative can be either positive or negative, depending on N. In fact, by taking the derivative of Eq. (13) and setting $R = 0$ one gets

$$\frac{\partial\langle T_f\rangle^{(A)}(R,N)}{\partial R}\Big|_{R=0} = N\int_0^{+\infty}[q(0,T)]^{N-1}\frac{\partial q(R,T)}{\partial R}\Big|_{R=0}dT, \tag{16}$$

where, using Eq. (8), one has

$$q(0,T) = \mathrm{erf}\left(\frac{1}{\sqrt{4\,T}}\right). \tag{17}$$

Taking the derivative of Eq. (12) with respect to R and setting $R = 0$ gives

$$\frac{\partial q(R,T)}{\partial R}\Big|_{R=0} = \int_\Gamma \frac{dS}{2\pi i}\,e^{ST}\left[\frac{1}{2\,S^{3/2}}\,e^{-\sqrt{S}} - \frac{1}{S^2}\,(e^{-\sqrt{S}} - e^{-2\sqrt{S}})\right]. \tag{18}$$

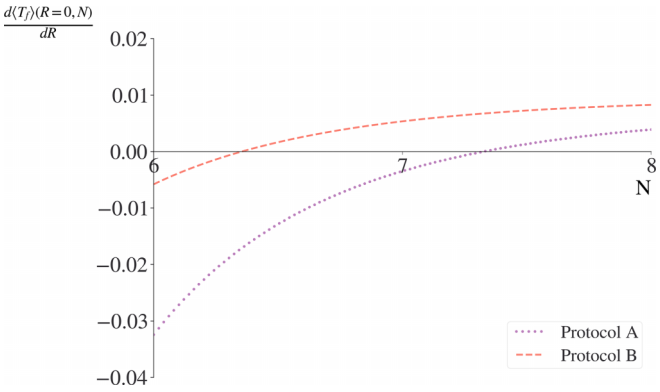

FIG. 3. The derivative of the MFPT at $R = 0$ in Eq. (16) (protocol A) and Eq. (29) (protocol B), plotted as a function of N for $6 < N < 8$. The derivatives change sign respectively at $N_c = 7.3264773\ldots$ (protocol A) and $N_c = 6.3555864\ldots$ (protocol B).

This Laplace inversion can be explicitly done to give

$$\left.\frac{\partial q(R,T)}{\partial R}\right|_{R=0} = (T+1)\,\mathrm{erf}\left(\frac{1}{\sqrt{4\,T}}\right) - (T+2)\,\mathrm{erf}\left(\frac{1}{\sqrt{T}}\right) + \frac{2\sqrt{T}}{\sqrt{\pi}}\left(e^{-\frac{1}{4T}} - e^{-\frac{1}{T}}\right) + 1. \tag{19}$$

Plugging Eqs. (17) and (19) in Eq. (16) gives us the derivative of the MFPT at $R = 0$ in terms of a single integral, which unfortunately is not easy to evaluate explicitly. However, it can be easily evaluated numerically for all $N > 4$ using *Mathematica* (see Fig. 3). As N increases beyond 4, the derivative at $R = 0$ in Eq. (16) increases, being negative initially, as can be seen in Fig. 3. As long as this derivative at $R = 0$ is negative, we have a nonzero $R^* > 0$. When the derivative changes sign and becomes positive, we have $R^* = 0$. Using a dichotomous algorithm, we find that this change of sign occurs at $N_c = 7.3264773\ldots$. This is our main result in this section. It says that the resetting in protocol A is beneficial for a team of N searchers as long as $N < N_c$. When $N > N_c$, resetting increases the search time and hence is no longer a useful strategy.

IV. PROTOCOL B

In protocol B the *simultaneous* resetting (see the right panel of Fig. 1) induces strong long-range correlations between the walkers [45]. Hence, the system is not simply N independent copies of a single resetting random walker. However, since the resetting happens *simultaneously* we have a new renewal equation for the N-particle stochastic process:

$$S^{(B)}_{r,N}(x_0,t) = e^{-rt}\,S^{(B)}_{0,N}(x_0,t) + r\int_0^{+\infty} d\tau\; e^{-r\tau}\,S^{(B)}_{0,N}(x_0,\tau)\,S^{(B)}_{r,N}(x_0,t-\tau). \tag{20}$$

The explanation of this renewal equation is exactly similar to Eq. (5), except that one has to think in terms of an N-particle process as a whole. Now note that without resetting, i.e., for $r = 0$, the walkers become independent, and hence using Eq. (8) we have

$$S^{(B)}_{0,N}(x_0,t) = [Q_0(x_0,t)]^N = \left[\mathrm{erf}\left(\frac{x_0}{\sqrt{4Dt}}\right)\right]^N. \tag{21}$$

As was done in Eq. (5), taking the Laplace transform of Eq. (20) we obtain

$$\tilde{S}^{(B)}_{r,N}(x_0,s) = \frac{\tilde{S}^{(B)}_{0,N}(x_0,s+r)}{1 - r\tilde{S}^{(B)}_{0,N}(x_0,s+r)}. \tag{22}$$

Finally using Eq. (3) we can express the MFPT as

$$\langle t_f\rangle^{(B)}_{r,N}(x_0) = \tilde{S}^{(B)}_{r,N}(x_0,s=0) = \frac{\tilde{S}^{(B)}_{0,N}(x_0,r)}{1 - r\tilde{S}^{(B)}_{0,N}(x_0,r)}. \tag{23}$$

Inserting Eq. (21) into Eq. (23) we then get an explicit formula

$$\langle t_f\rangle^{(B)}_{r,N}(x_0) = \frac{\int_0^{+\infty} dt\; e^{-rt}\left[\mathrm{erf}\left(\frac{x_0}{\sqrt{4Dt}}\right)\right]^N}{1 - r\int_0^{+\infty} dt\; e^{-rt}\left[\mathrm{erf}\left(\frac{x_0}{\sqrt{4Dt}}\right)\right]^N}. \tag{24}$$

Once again we appropriately rescale the variables to make them dimensionless by setting $T = \frac{D}{x_0^2}t$ and $R = \frac{x_0^2}{D}r$ and obtain the simpler expression

$$\langle T_f\rangle^{(B)}(R,N) = \frac{D}{x_0^2}\langle t_f\rangle^{(B)}_{r,N}(x_0) = \frac{\int_0^{+\infty} dT\; e^{-RT}\left[\mathrm{erf}\left(\frac{1}{\sqrt{4T}}\right)\right]^N}{1 - R\int_0^{+\infty} dT\; e^{-RT}\left[\mathrm{erf}\left(\frac{1}{\sqrt{4T}}\right)\right]^N} = \frac{h(R,N)}{1 - R\,h(R,N)}, \tag{25}$$

where for simplicity we introduced the function

$$h(R,N) = \int_0^{+\infty} dT\; e^{-RT}\left[\mathrm{erf}\left(\frac{1}{\sqrt{4T}}\right)\right]^N. \tag{26}$$

We verify this theoretical result by comparing it to numerical Langevin simulations as shown in the right panel of Fig. 2. As in the case of protocol A, we infer the existence or not of a nonzero optimal $R^* > 0$ by analyzing the small R behavior of Eq. (25). The detailed derivation of the small R behavior for different N is given in Appendix B. Here we summarize these results:

$$\langle T_f\rangle^{(B)}(R,N) \overset{R\ll 1}{\sim} \begin{cases} \frac{\Gamma(1-N/2)}{\pi^{N/2}}\frac{1}{R^{1-N/2}} & \text{if } N<2 \\ -\frac{1}{\pi}\ln R & \text{if } N=2 \\ C_N^{(B)} - \frac{\Gamma(2-N/2)(2-N/2)}{\pi^{N/2}}R^{N/2-1} & \text{if } 2<N<4 \\ C_N^{(B)} + \frac{1}{\pi^2}R\ln R & \text{if } N=4 \\ C_N^{(B)} + \left\{\left[\int_0^{+\infty}\left[\mathrm{erf}\left(\frac{1}{\sqrt{4T}}\right)\right]^N dT\right]^2 - \int_0^{+\infty} T\left[\mathrm{erf}\left(\frac{1}{\sqrt{4T}}\right)\right]^N dT\right\}R & \text{if } N>4, \end{cases} \tag{27}$$

where for any $N > 2$, $C_N^{(B)}$ is a constant given by

$$C_N^{(B)} = \langle T_f\rangle^{(B)}(0,N) = \langle T_f\rangle^{(A)}(0,N) = \int_0^{+\infty}\left[\mathrm{erf}\left(\frac{1}{\sqrt{4T}}\right)\right]^N dT. \tag{28}$$

As in the case of protocol A, it is clear from the small R behavior that there is an optimal $R^* > 0$ for all $N \leqslant 4$. For $N > 4$, both $h(R,N)$ and its first derivative are convergent when $R \to 0$. Then the derivative of the MFPT, for $N > 4$, is given by

$$\left.\frac{\partial\langle T_f\rangle^{(B)}(R,N)}{\partial R}\right|_{R=0} = [h(0,N)]^2 + \partial_R h(R,N)\Big|_{R=0} = \left\{\int_0^{+\infty}\left[\mathrm{erf}\left(\frac{1}{\sqrt{4T}}\right)\right]^N dT\right\}^2 - \int_0^{+\infty} T\left[\mathrm{erf}\left(\frac{1}{\sqrt{4T}}\right)\right]^N dT. \tag{29}$$

The existence of a finite $R^\star > 0$ is uniquely determined by the sign of the above expression. If it is negative, then there exists a finite $R^\star > 0$. However, if it is positive, then $R^\star = 0$ and the resetting hinders the search process. Once again, the integrals in Eq. (29) can be easily evaluated using *Mathematica* (see Fig. 3), and we find that the critical value of N defined as the value for which the derivative of the MFPT at $R = 0$ changes sign is given by $N_c = 6.3555864\ldots$. Thus, for protocol B, resetting benefits the search process as long as $N < N_c$, but delays the search process for $N > N_c$.

The value of N_c is slightly smaller in protocol B than that of protocol A. It is not easy to guess these values of N_c *a priori* from simple physical arguments. However, one can understand why the value of N_c for protocol B is lower than that of protocol A from the following argument. As was shown in [46] in protocol B the simultaneous resetting induces an effective attraction between all the particles. The simultaneous resetting pulls the particles together. Hence protocol B not only restricts the movement of the particles to stay closer to the origin, but it also creates coordination between the particles further constraining the movement of the ensemble of particles. Therefore, the constraints of protocol B are stronger than those of protocol A leading to resetting becoming inefficient faster for protocol B, which in turn leads to a lower value of N_c.

V. CONCLUSION

To summarize, in this paper we have studied analytically the mean first-passage time to a target at the origin in one dimension by N Brownian walkers all starting at $x_0 > 0$ and undergoing diffusion with stochastic resetting. We considered two resetting protocols: (A) where each walker diffuses and resets to x_0 with rate *rindependently* and (B) each walker diffuses independently but resets *simultaneously* to x_0 with rate r. While in protocol A, the walkers remain *uncorrelated* at all times, in protocol B they become strongly *correlated* dynamically via simultaneous resetting. We showed that in both protocols, the mean first-passage time, as a function of the resetting rate r, has a minimum at $r = r^* > 0$ as long as $N < N_c$, but for $N > N_c$ the optimal resetting rate is $r^* = 0$. The value of N_c is slightly different in the two protocols. Continuing our results analytically to real N, we showed that $N_c = 7.3264773\ldots$ for protocol A, while $N_c = 6.3555864\ldots$ for protocol B. The main conclusion of our work is that resetting is beneficial for the search process only when $N < N_c$. For $N > N_c$, resetting hinders the search process. Our analytical results have been verified in numerical Langevin simulations.

The mean first-passage time for a single $N = 1$ walker has already been measured in optical tweezer experiments in one [32,33] and two dimensions [34]. It would be interesting to see if these measurements can be extended to the $N > 1$ case presented here, and in particular to verify our theoretical predictions for N_c in the two protocols.

There are a number of other interesting directions in which our work may be extended. A study of higher-order cumulants of the first-passage time, beyond the mean, might reveal other interesting differences between the two protocols. It would also be interesting to find the critical values N_c in higher dimensions for both resetting protocols. Finally, one may investigate the mean first-passage time for interacting walkers and for nondiffusive processes such as Lévy flights, using both resetting protocols.

APPENDIX A: PROTOCOL A

In these Appendixes we provide a detailed derivation of the small R behavior of the scaled MFPT $\langle T_f\rangle^{(A,B)}(R,N)$ for different values of $0 < N \leqslant 4$. The results for protocols A and B are derived separately in the two following Appendixes. In Appendix C we provide some numerical details.

For protocol A, the MFPT is given by Eq. (13), which reads

$$\langle T_f\rangle^{(A)}(R,N)=\int_0^{+\infty}[q(R,T)]^N\,dT, \tag{A1}$$

where

$$q(R,T)=\int_\Gamma \frac{dS}{2\pi i}\,e^{ST}\,\frac{1-e^{-\sqrt{S+R}}}{S+R\,e^{-\sqrt{S+R}}}. \tag{A2}$$

In particular,

$$q(0,T)=\mathrm{erf}\left(\frac{1}{\sqrt{4\,T}}\right). \tag{A3}$$

Now, if we put $R=0$ in Eq. (A1) and use Eq. (A3), we get

$$\langle T_f\rangle^{(A)}(0,N)=\int_0^{\infty}\left[\mathrm{erf}\left(\frac{1}{\sqrt{4\,T}}\right)\right]^N dT. \tag{A4}$$

Using $\mathrm{erf}(z)\approx(2/\sqrt{\pi})\,z$ as $z\to 0$, one finds that the integrand in Eq. (A4) behaves as $T^{-N/2}$ for large T. Hence the integral is convergent for $N>2$ but diverges for $N\leqslant 2$. This divergence for $N\leqslant 2$ stems from the large T behavior of the integrand. This indicates that the behavior near $R=0$ depends crucially on N and is delicate to extract analytically. Since the divergence at $R=0$ comes from the large T behavior of the integrand for $N\leqslant 2$, in order to extract the leading singular behavior of the MFPT near $R=0$, it is necessary to investigate the scaling limit of $q(R,T)$ in Eq. (A2) when $R\to 0$, $T\to\infty$ while keeping the product RT fixed. One can then substitute this scaling form of $q(R,T)$ in Eq. (A1) and investigate the singular behavior of the MFPT as $R\to 0$.

To extract the scaling behavior of $q(R,T)$, we take the limit $R\to 0$ and $S\to 0$ in Eq. (A2), while keeping the ratio $\tilde{S}=S/R$ fixed. Keeping $z=R\,T$ fixed, we get to leading order for small R

$$q(R,T)\approx\frac{1}{\sqrt{R}}\int_\Gamma\frac{d\tilde{S}}{2\pi i}\,e^{\tilde{S}z}\,\frac{1}{\sqrt{1+\tilde{S}}}=\frac{1}{\sqrt{\pi\,R\,z}}\,e^{-z}. \tag{A5}$$

Consequently, in this scaling limit, we have

$$q(R,T)\approx\frac{1}{\sqrt{T}}\,f(R\,T),\qquad\text{where}\qquad f(z)=\frac{1}{\sqrt{\pi}}\,e^{-z}. \tag{A6}$$

Substituting this leading scaling behavior of $q(R,T)$ in Eq. (A1), we then compute the small R behavior of the MFPT. Below we treat the five different cases $N<2$, $N=2$, $2<N<4$, $N=4$, and $N>4$ separately in five subsections.

1. The case $N<2$

In this case, substituting the scaling form of $q(R,T)$ from Eq. (A6) in Eq. (A1), we get

$$\begin{aligned}\langle T_f\rangle^{(A)}(R,N)&\approx\int_0^{+\infty}\left[\frac{1}{\sqrt{T}}f(RT)\right]^N dT\\&=\frac{R^{N/2-1}}{\pi^{N/2}}\int_0^{+\infty}e^{-Nu}u^{-N/2}du\\&=\frac{\Gamma(1-N/2)}{\pi^{N/2}}\,N^{N/2-1}\,R^{N/2-1}.\end{aligned} \tag{A7}$$

Hence we see that, as long as $N<2$, the integral converges in Eq. (A7) and the MFPT diverges as $\sim R^{N/2-1}$ as $R\to 0$.

2. The case $N=2$

In the $N=2$ case we have to be a bit more careful. To start, we split the integral in Eq. (A1) into three regions: $T\in[0,1]$, $T\in[1,1/R]$, and $T\in[1/R,\infty)$. In the third part where T is large, we can approximate $q(R,T)$ by its scaling form in Eq. (A6). This gives

$$\begin{aligned}\langle T_f\rangle^{(A)}(R,N)\approx&\int_0^1[q(R,T)]^2\,dT+\int_1^{1/R}[q(R,T)]^2\,dT\\&+\int_{1/R}^{+\infty}\frac{1}{T}\,[f(RT)]^2dT.\end{aligned} \tag{A8}$$

Changing the variable to $z=RT$ in the third integral, we see that it is $O(1)$ since $f(z)=e^{-z}/\sqrt{\pi}$. Hence

$$\begin{aligned}\langle T_f\rangle^{(A)}(R,N)\approx&\int_0^1[q(R,T)]^2\,dT\\&+\int_1^{1/R}[q(R,T)]^2\,dT+O(1).\end{aligned} \tag{A9}$$

For $T\ll 1/R$, the process is typically not resetting, and hence we can replace $q(R,T)\approx q(0,T)=\mathrm{erf}(1/\sqrt{4T})$ in the first two integrals. This gives

$$\begin{aligned}\langle T_f\rangle^{(A)}(R,N)\approx&\int_0^1 dT\left[\mathrm{erf}\left(\frac{1}{\sqrt{4T}}\right)\right]^2\\&+\int_1^{1/R}dT\left[\mathrm{erf}\left(\frac{1}{\sqrt{4T}}\right)\right]^2+O(1).\end{aligned} \tag{A10}$$

The first integral is clearly $O(1)$, and the principal divergence comes from the second integral, which is dominated by the integrand near the upper limit $1/R$. Since $T\gg 1$, we can now expand $\mathrm{erf}(1/\sqrt{4T})$ as a power series in $1/\sqrt{T}$. The first term gives $\mathrm{erf}(1/\sqrt{4T})\approx 1/\sqrt{\pi\,T}$. Substituting this behavior in the second integral in Eq. (A10) gives the leading order divergence

$$\langle T_f\rangle^{(A)}(R,N)\approx\frac{1}{\pi}\int_1^{1/R}\frac{dT}{T}+O(1)=-\frac{1}{\pi}\ln R+O(1). \tag{A11}$$

3. The case $2<N<4$

In this case the integral in Eq. (A1) is convergent for $R=0$ and is given by Eq. (A4). However, the subleading term turns out to be singular as $R\to 0$. To derive the subleading term, it is useful to analyze the derivative at $R=0$. Indeed, deriving Eq. (A1) with respect to R gives

$$\frac{\partial\langle T_f\rangle^{(A)}(R,N)}{\partial R}=N\int_0^{+\infty}[q(R,T)]^{N-1}\,\frac{\partial q(R,T)}{\partial R}\,dT. \tag{A12}$$

Now we replace $q(R,T)$ by its scaling form in Eq. (A6) and make the change of variable $z=RT$. This gives

$$\frac{\partial\langle T_f\rangle^{(A)}(R,N)}{\partial R}\approx N\,R^{N/2-2}\int_0^{+\infty}z^{1-N/2}\,[f(z)]^{N-1}\,f'(z)\,dz. \tag{A13}$$

Using $f(z) = e^{-z}/\sqrt{\pi}$ and performing the integral exactly gives

$$\frac{\partial \langle T_f \rangle^{(A)}(R,N)}{\partial R} \approx -\frac{\Gamma(2-N/2)}{\pi^{N/2}} \Gamma(2-N/2)\, R^{N/2-2}. \quad \text{(A14)}$$

Note that this is well defined for $N < 4$; otherwise the Gamma function is diverging. Integrating it back with respect to R gives the small R asymptotic behavior of the MFPT

$$\langle T_f \rangle^{(A)}(R,N) \approx \int_0^\infty \left[\mathrm{erf}\left(\frac{1}{\sqrt{4T}}\right)\right]^N dT - \frac{2\,\Gamma(2-N/2)}{(N-2)\,\pi^{N/2}} N^{N/2-1}\, R^{N/2-1}. \quad \text{(A15)}$$

Clearly as R increases from 0, the MFPT decreases due to the negative sign of the second term in Eq. (A15), indicating that the minimum of the MFPT occurs at $R^* > 0$.

4. The case $N = 4$

In the $N = 4$ case, the analysis is somewhat similar to the $N = 2$ case. In this case the derivative in Eq. (A12) reads

$$\frac{\partial \langle T_f \rangle^{(A)}(R,4)}{\partial R} = 4 \int_0^{+\infty} [q(R,T)]^3 \frac{\partial q(R,T)}{\partial R}\, dT. \quad \text{(A16)}$$

We anticipate in this case, and verify *a posteriori*, that as in the case $N = 2$, the scaling form of $q(R,T)$ gives only a $O(1)$ contribution, and the leading divergence as $R \to 0$ in Eq. (A16) has a different source. So we need to go beyond the scaling regime and estimate both $q(R,T)$ and $\partial_R q(R,T)$ for small R. The first one is simple since we already know explicitly that $q(0,T) = \mathrm{erf}(1/\sqrt{4T})$. To estimate the derivative for small R, we note that for $T \ll 1/R$, the diffusing particle typically hardly resets and hence

$$q(R,T) \approx e^{-RT} q(0,T) \approx q(0,T) - R\,T\, q(0,T). \quad \text{(A17)}$$

Taking a derivative with respect to R gives the estimate

$$\frac{\partial q(R,T)}{\partial R} \approx -T\, e^{-RT}\, q(0,T) \sim -T\, q(0,T). \quad \text{(A18)}$$

To proceed, we now split the integral in Eq. (A16) into three regimes: [0,1], [1, $1/R$], and [$1/R$, ∞),

$$\frac{\partial \langle T_f \rangle^{(A)}(R,4)}{\partial R} = 4 \int_0^1 [q(R,T)]^3 \frac{\partial q(R,T)}{\partial R}\, dT + 4 \int_1^{1/R} [q(R,T)]^3 \frac{\partial q(R,T)}{\partial R}\, dT + 4 \int_{1/R}^{\infty} [q(R,T)]^3 \frac{\partial q(R,T)}{\partial R}\, dT. \quad \text{(A19)}$$

In the third integral, denoted by I_3, we can use the scaling form of $q(R,T)$ in Eq. (A6) and get, after the customary change of variables $z = RT$,

$$I_3 \approx 4 \int_1^\infty \frac{dz}{z} [f(z)]^3 f'(z) \sim O(1), \quad \text{(A20)}$$

where we used $f(z) = e^{-z}/\sqrt{\pi}$. In the first two integrals, in contrast, we cannot use the scaling form. Instead, we can replace $q(R,T)$ and $\partial_R q(R,T)$ by their approximate forms in Eqs. (A17) and (A18), respectively. It is easy to check that after this substitution, the first integral I_1 over [0,1] in Eq. (A19) is $O(1)$. Hence the leading divergence in Eq. (A19) comes from the second integral I_2 over [1, $1/R$], which then reads

$$I_2 \approx 4 \int_1^{1/R} [q(0,T]^3\, [-T\, q(0,T)]\, dT = -4 \int_1^{1/R} T \left[\mathrm{erf}\left(\frac{1}{\sqrt{4T}}\right)\right]^4 dT. \quad \text{(A21)}$$

In this range, since $T \gg 1$, we can again expand $\mathrm{erf}(1/\sqrt{4T})$ in a Taylor series in powers of $1/\sqrt{T}$. The first term in this expansion provides the leading divergence, and we get

$$I_2 \approx \frac{4}{\pi^2} \int_1^{1/R} \frac{dT}{T} \approx \frac{4}{\pi^2} \ln R. \quad \text{(A22)}$$

Adding the three integrals, we then find that as $R \to 0$

$$\frac{\partial \langle T_f \rangle^{(A)}(R,4)}{\partial R} \approx \frac{4}{\pi^2} \ln R + O(1). \quad \text{(A23)}$$

Integrating back with respect to R, we then get the leading small R behavior of the MFPT

$$\langle T_f \rangle^{(A)}(R,4) \approx \int_0^\infty \left[\mathrm{erf}\left(\frac{1}{\sqrt{4T}}\right)\right]^4 dT + \frac{4}{\pi^2} R \ln R. \quad \text{(A24)}$$

Note that the subleading term is negative for small R, indicating that the MFPT decreases from its $R = 0$ value as R increases. This again implies that the MFPT has a nonzero minimum at some $R^* > 0$.

5. The case $N > 4$

Finally, in the fifth case when $N > 4$, both the MFPT and its first derivative are finite at $R = 0$. Hence, the subleading behavior for $N > 4$ is linear as $R \to 0$. As discussed in the main text, the sign of the subleading linear term changes from negative to positive as N crosses $N_c = 7.7.3264773\ldots$ from below.

The different behaviors of $\langle T_f \rangle^{(A)}(R,N)$ for small R are summarized in Eq. (14).

APPENDIX B: PROTOCOL B

For protocol B, we recall that the MFPT is given by Eq. (25), namely,

$$\langle T_f \rangle^{(B)}(R,N) = \frac{h(R,N)}{1 - R\,h(R,N)}, \quad \text{(B1)}$$

where the function $h(R,N)$, given in Eq. (26), reads

$$h(R,N) = \int_0^{+\infty} dT\, e^{-RT} \left[\mathrm{erf}\left(\frac{1}{\sqrt{4T}}\right)\right]^N. \quad \text{(B2)}$$

It is convenient to make a change of variable $u = R\,T$ in Eq. (B2) and rewrite it as

$$h(R,N) = \frac{1}{R} \int_0^{+\infty} du\, e^{-u} \left[\mathrm{erf}\left(\sqrt{\frac{R}{4u}}\right)\right]^N. \quad \text{(B3)}$$

Putting directly $R = 0$ in Eq. (B1) gives the same result as in Eq. (A4) for protocol A, namely,

$$\langle T_f\rangle^{(B)}(0,N) = h(0,N) = \int_0^\infty \left[\mathrm{erf}\left(\frac{1}{\sqrt{4\,T}}\right)\right]^N dT. \quad \text{(B4)}$$

Again this integral is convergent only for $N > 2$.

For later purposes, we will also need the first derivative of $h(R,N)$ with respect to R, which reads from Eq. (B2)

$$\frac{\partial h(R,N)}{\partial R} = -\int_0^{+\infty} dT\, T\, e^{-RT}\left[\mathrm{erf}\left(\frac{1}{\sqrt{4T}}\right)\right]^N. \quad \text{(B5)}$$

Performing the same change of variable $u = RT$, one obtains an alternative expression

$$\frac{\partial h(R,N)}{\partial R} = -\frac{1}{R^2}\int_0^{+\infty} du\, u\, e^{-u}\left[\mathrm{erf}\left(\sqrt{\frac{R}{4u}}\right)\right]^N. \quad \text{(B6)}$$

Our goal is to extract the asymptotic small R behavior of $h(R,N)$ in Eq. (B2) or equivalently in Eq. (B3) for different N and then use these results in Eq. (B1) to derive the small R behavior of the MFPT. As in protocol A, we consider the five cases $N < 2, N = 2, 2 < N < 4, N = 4$ and $N > 4$ separately in the five subsections below.

1. The case $N < 2$

When $N < 2$ the integral $h(R,N)$ in Eq. (B3) becomes divergent as $R \to 0$ and the divergence ensues from the large u regime of the integrand. To compute this small R divergence, we use $\mathrm{erf}(z) \approx (2/\sqrt{\pi})\,z$ for small z in Eq. (B3) and carry out the integral. This gives, to leading order as $R \to 0$,

$$h(R,N) \approx \frac{R^{N/2-1}}{\pi^{N/2}}\int_0^{+\infty} e^{-u}\,u^{-N/2}\,du = \frac{\Gamma(1-N/2)}{\pi^{N/2}}\,R^{N/2-1}. \quad \text{(B7)}$$

Note that this result is valid only for $N < 2$, as otherwise the Gamma function becomes divergent. Substituting this behavior of $h(R,N)$ in Eq. (B1) we get, to leading order for small R,

$$\langle T_f\rangle^{(B)}(R,N) \approx \frac{\Gamma(1-N/2)}{\pi^{N/2}}\,\frac{1}{R^{1-N/2}}. \quad \text{(B8)}$$

This divergence of the MFPT as $R \to 0$, along with its divergence as $R \to \infty$, indicates that the minimum of the MFPT occurs at a nonzero $R^* > 0$ for $N < 2$.

2. The case $N = 2$

For $N = 2$ we need to make a finer analysis of $h(R,N)$. In this case we split the integral in Eq. (B3) into two regimes: $u < R \ll 1$ and $u > R$. This leads to

$$h(R,2) = \frac{1}{R}\int_0^R du\, e^{-u}\left[\mathrm{erf}\left(\sqrt{\frac{R}{4u}}\right)\right]^2 + \frac{1}{R}\int_R^{+\infty} du\, e^{-u}\left[\mathrm{erf}\left(\sqrt{\frac{R}{4u}}\right)\right]^2. \quad \text{(B9)}$$

Then in the integrand in the first term, to leading order, the erf function can be replaced by 1, and hence the integral remains $O(1)$ as $R \to 0$. The divergence comes from the second integral, where we can use $\mathrm{erf}(z) \approx (2/\sqrt{\pi})\,z$ for small z. This gives

$$h(R,N) \approx \frac{1}{\pi}\int_R^{+\infty}\frac{du}{u}\,e^{-u} + O(1). \quad \text{(B10)}$$

Integrating by parts, one immediately finds the leading order behavior for small R,

$$h(R,N) \approx -\frac{1}{\pi}\,\ln R + O(1). \quad \text{(B11)}$$

Finally, substituting this in Eq. (B1), we get

$$\langle T_f\rangle^{(B)}(R,2) \approx -\frac{1}{\pi}\,\ln R + O(1). \quad \text{(B12)}$$

Hence, the MFPT diverges logarithmically as $R \to 0$, indicating that for $N = 2$, we will again have a nonzero R^*.

3. The case $2 < N < 4$

For $N > 2$, putting $R = 0$ in Eq. (B2), one finds that $h(0,N)$ is finite and is given by Eq. (B4). Hence $\langle T_f\rangle^{(B)}(0,N) = h(0,N) < +\infty$ from Eq. (B1). To extract the dominant subleading term, it is convenient to first find how the derivative of $h(R,N)$ diverges as $R \to 0$ by analyzing Eq. (B5) or equivalently Eq. (B6). We insert the asymptotic small z behavior $\mathrm{erf}(z) \approx (2/\sqrt{\pi})\,z$ in Eq. (B6) to get the leading small R behavior

$$\frac{\partial h(R,N)}{\partial R} \approx -\frac{R^{N/2-2}}{\pi^{N/2}}\int_0^{+\infty} du\, e^{-u}\,u^{1-N/2} = -\frac{\Gamma(2-N/2)}{\pi^{N/2}}\,R^{N/2-2}. \quad \text{(B13)}$$

Note that the Gamma function is well defined for $N < 4$. Integrating it back with respect to R, we then get, up to the first subleading term,

$$h(R,N) \approx h(0,N) - \frac{2\,\Gamma(2-N/2)}{(N-2)\,\pi^{N/2}}\,R^{N/2-1}. \quad \text{(B14)}$$

Finally, substituting this result for $h(R,N)$ in Eq. (B1) we get, noting that $(N/2-1) < 1$, the following result:

$$\langle T_f\rangle^{(B)}(R,N) \approx h(R,N) \approx h(0,N) - \frac{2\,\Gamma(2-N/2)}{(N-2)\,\pi^{N/2}}\,R^{N/2-1}. \quad \text{(B15)}$$

Note that the subleading term is negative for $2 < N < 4$, indicating that the MFPT decreases from its value at $R = 0$ as R increases. This again implies that the optimal $R^* > 0$.

4. The case $N = 4$

In this case $h(0, 4)$ in Eq. (B2) is finite. To extract the subleading behavior as $R \to 0$, we again analyze the derivative in Eq. (B6) by splitting the integral into two regimes $u < R \ll 1$ and $u > R$

$$\frac{\partial h(R,4)}{\partial R} = -\frac{1}{R^2}\int_0^R du\, u\, e^{-u}\left[\mathrm{erf}\left(\sqrt{\frac{R}{4u}}\right)\right]^4 - \frac{1}{R^2}\int_R^{+\infty} du\, u\, e^{-u}\left[\mathrm{erf}\left(\sqrt{\frac{R}{4u}}\right)\right]^4. \quad \text{(B16)}$$

We can replace the erf by 1 in the integrand in the first term, leading to an $O(1)$ result for the first integral as $R \to 0$. In the second integral, we use the small z behavior of the error function $\mathrm{erf}(z) \approx (2/\sqrt{\pi})\, z$, which then gives

$$\frac{\partial h(R,4)}{\partial R} \approx O(1) - \frac{1}{\pi^2}\int_R^{\infty} \frac{du}{u}\, e^{-u}. \quad \text{(B17)}$$

Integrating by parts, one gets the leading order behavior for small R,

$$\frac{\partial h(R,4)}{\partial R} \approx \frac{1}{\pi^2}\ln R. \quad \text{(B18)}$$

Integrating it back with respect to R gives

$$h(R,4) \approx h(0,4) + \frac{1}{\pi^2} R \ln R. \quad \text{(B19)}$$

Finally, substituting this result in Eq. (B1) gives the small R asymptotics of the MFPT

$$\langle T_f\rangle^{(B)}(R,4) \approx h(0,4) + \frac{1}{\pi^2} R \ln R. \quad \text{(B20)}$$

Since the second term is negative as $R \to 0$, we again see that the MFPT decreases from its value at $R = 0$ as R increases, indicating that the optimal $R^* > 0$.

5. The case $N > 4$

Finally, in the fifth case when $N > 4$, both $h(0, N)$ in Eq. (B2) and its first derivative $h'(0, N)$ in Eq. (B5) are finite. Expanding Eq. (B1) up to $O(R)$, we then get as $R \to 0$

$$\langle T_f\rangle^{(B)}(R,N) \approx h(0,N) + \left[h(0,N + h'(0,N)\right] R = \int_0^{\infty}\left[\mathrm{erf}\left(\frac{1}{\sqrt{4\,T}}\right)\right]^N dT + \left(\left\{\int_0^{+\infty}\left[\mathrm{erf}\left(\frac{1}{\sqrt{4T}}\right)\right]^N dT\right\}^2 - \int_0^{+\infty} T\left[\mathrm{erf}\left(\frac{1}{\sqrt{4T}}\right)\right]^N dT\right) R. \quad \text{(B21)}$$

Hence, the subleading behavior of the MFPT for $N > 4$ is linear as $R \to 0$, as in protocol A. The sign of the subleading linear term is negative for $N < N_c$ and is positive for $N > N_c$ where $N_c = 6.3555864\ldots$.

The different behaviors of $\langle T_f\rangle^{(B)}(R, N)$ for small R are summarized in Eq. (27).

APPENDIX C: NUMERICAL DETAILS

The numerical results in this paper were obtained by numerical Langevin simulations, where we simulate numerically the evolution of either protocol A or protocol B in discrete time and space by making microscopic discrete jumps or long resetting motions at fixed microscopic time intervals. In practice, we by initializing a vector of positions $\vec{x}(t) = (x_1(t), x_2(t), \ldots, x_N(t)) = (0, 0, \ldots, 0)$. We then make the system evolve according to the following rule for protocol A

$$\text{For every } i \text{ from 1 to } N, \quad x_i(t+dt) = \begin{cases} 0 & \text{with probability } r\,dt \\ x_i(t) + \eta_i(t) & \text{with probability } 1 - r\,dt \end{cases}, \quad \text{(C1)}$$

and respectively for protocol B

$$\vec{x}(t+dt) = \begin{cases} (0, 0, \ldots, 0) & \text{with probability } r\,dt \\ [x_1(t) + \eta_1(t), x_2(t) + \eta_2(t), \ldots, x_N(t) + \eta_N(t)] & \text{with probability } 1 - r\,dt \end{cases}, \quad \text{(C2)}$$

where the variables $\eta_i(t)$ are random Gaussian numbers such that $\langle \eta_i(n_1 dt)\eta_j(n_2 dt)\rangle = 2D dt\, \delta_{ij}\delta_{n_1 n_2}$. We then let the system evolve for 3 million time steps, where the step size is given by $dt = 10^{-5}$. We interrupt the evolution as soon as one of the variables $x_i(t)$ crosses over a fixed target and we record the time at which this occurred, which is the first-passage time. We repeat this whole process 10^5 times and average all the obtained first-passage times to obtain the numerical first-passage time. The control parameters of our numerical experiments are the values of N, dt, D, r and the position of the target. For more details, the code used to produce the results can be found in [50].

Furthermore, to find the exact continuous value of N_c we use a dichotomous algorithm to find where the first derivative changes sign. This algorithm consists in starting from a lower and upper bound estimate L and U of the value of N_c. We compute

the first derivative of the MFPT evaluated at $r = 0$ for $N = L$ and check that it is negative, as well as computing the value of the function at $N = U$ and checking that it is positive. If this is the case, since we are dealing with continuous functions we know that the function must cancel for a certain $N_c \in [L, U]$. We can therefore proceed with the algorithm, and we compute the first derivative of the MFPT at the center of the interval $M = (L + U)/2$. If it is positive, then we know that $N_c \in [L, M[$, if it is negative, we know that $N_c \in]M, U]$, and if it is exactly 0, then $N_c = M$. We iterate this argument until we reach a desired precision; in our case we chose $U - L \sim 10^{-8} = \epsilon$, which gives us a value for N_c, which is accurate up to ϵ.

[1] W. J. Bell, *Searching Behaviour: The Behavioural Ecology of Finding Resources* (Chapman and Hall, London, 1991).

[2] G. Adam and M. Delbrück, Struct. Chem. Mol. Biol. **198**, 198 (1968).

[3] R. Metzler, S. Redner, and G. Oshanin, *First-Passage Phenomena and Their Applications* (World Scientific, Singapore, 2014), Vol. 35.

[4] F. Bartumeus and J. Catalan, J. Phys. A: Math. Theor. **42**, 434002 (2009).

[5] G. M. Viswanathan, M. G. E. da Luz, E. P. Raposo, and H. E. Stanley, *The Physics of Foraging: An Introduction to Random Searches and Biological Encounters* (Cambridge University Press, Cambridge, 2011).

[6] O. G. Berg, R. B. Winter, and P. H. von Hippel, Biochemistry **20**, 6929 (1981).

[7] M. Coppey, O. Bénichou, and M. Moreau, Biophys. J. **87**, 1640 (2004).

[8] S. Ghosh, B. Mishra, A. B. Kolomeisky, and D. Chowdhury, J. Stat. Mech. (2018) 123209.

[9] D. Chowdhury, Biophys. J. **116**, 2057 (2019).

[10] O. Bénichou, M. Coppey, M. Moreau, P.-H. Suet, and R. Voituriez, Phys. Rev. Lett. **94**, 198101 (2005).

[11] O. Bénichou, M. Moreau, P.-H. Suet, and R. Voituriez, J. Chem. Phys. **126**, 234109 (2007).

[12] O. Bénichou, C. Loverdo, M. Moreau, and R. Voituriez, Rev. Mod. Phys. **83**, 81 (2011).

[13] M. Villen-Altramirano and J. Villen-Altramirano, in *Queueing, Performance and Control in ATM*, edited by J. W. Cohen and C. D. Pack (North-Holland, Amsterdam, 1991).

[14] M. Luby, A. Sinclair, and D. Zuckerman, Inf. Process. Lett. **47**, 173 (1993).

[15] H. Tong, C. Faloutsos, and J.-Y. Pan, Knowl. Inf. Syst. **14**, 327 (2008).

[16] J. H. Lorenz, in *SOFSEM 2018: Theory and Practice of Computer Science*, edited by A. Tjoa, L. Bellatreche, S. Biffl, J. van Leeuwen, and J. Wiedermann, Lecture Notes in Computer Science (Springer, Berlin, 2018).

[17] M. R. Evans, S. N. Majumdar, and G. Schehr, J. Phys. A: Math. Theor. **53**, 193001 (2020).

[18] M. R. Evans and S. N. Majumdar, Phys. Rev. Lett. **106**, 160601 (2011).

[19] M. R. Evans and S. N. Majumdar, J. Phys. A: Math. Theor. **44**, 435001 (2011).

[20] M. R. Evans and S. N. Majumdar, J. Phys. A: Math. Theor. **47**, 285001 (2014).

[21] L. Kusmierz, S. N. Majumdar, S. Sabhapandit, and G. Schehr, Phys. Rev. Lett. **113**, 220602 (2014).

[22] S. N. Majumdar, S. Sabhapandit, and G. Schehr, Phys. Rev. E **91**, 052131 (2015).

[23] A. Pal, A. Kundu, and M. R. Evans, J. Phys. A: Math. Theor. **49**, 225001 (2016).

[24] S. Reuveni, Phys. Rev. Lett. **116**, 170601 (2016).

[25] M. Montero and J. Villarroel, Phys. Rev. E **94**, 032132 (2016).

[26] A. Pal and S. Reuveni, Phys. Rev. Lett. **118**, 030603 (2017).

[27] D. Boyer, M. R. Evans, and S. N. Majumdar, J. Stat. Mech. (2017) 023208.

[28] A. Chechkin and I. M. Sokolov, Phys. Rev. Lett. **121**, 050601 (2018).

[29] P. C. Bressloff, J. Phys. A: Math. Theor. **53**, 425001 (2020).

[30] R. G. Pinsky, Stochastic Proc. Appl. **130**, 2954 (2020).

[31] B. De Bruyne, S. N. Majumdar, and G. Schehr, Phys. Rev. Lett. **128**, 200603 (2022).

[32] O. Tal-Friedman, A. Pal, A. Sekhon, S. Reuveni, and Y. Roichman, J. Phys. Chem. Lett. **11**, 7350 (2020).

[33] B. Besga, A. Bovon, A. Petrosyan, S. N. Majumdar, and S. Ciliberto, Phys. Rev. Res. **2**, 032029(R) (2020).

[34] F. Faisant, B. Besga, A. Petrosyan, S. Ciliberto, and S. N. Majumdar, J. Stat. Mech. (2021) 113203.

[35] C. Christou and A. Schadschneider, J. Phys. A: Math. Theor. **48**, 285003 (2015).

[36] D. Campos and V. Méndez, Phys. Rev. E **92**, 062115 (2015).

[37] S. Belan, Phys. Rev. Lett. **120**, 080601 (2018).

[38] S. Ray, D. Mondal, and S. Reuveni, J. Phys. A: Math. Theor. **52**, 255002 (2019).

[39] S. Ahmad, I. Nayak, A. Bansal, A. Nandi, and D. Das, Phys. Rev. E **99**, 022130 (2019).

[40] A. Pal and V. V. Prasad, Phys. Rev. Res. **1**, 032001(R) (2019).

[41] A. Pal and V. V. Prasad, Phys. Rev. E **99**, 032123 (2019).

[42] G. Mercado-Vásquez, D. Boyer, S. N. Majumdar, and G. Schehr, J. Stat. Mech. (2020) 113203.

[43] G. Mercado-Vásquez, D. Boyer, and S. N. Majumdar, J. Stat. Mech. (2022) 063203.

[44] G. Mercado-Vásquez, D. Boyer, and S. N. Majumdar, J. Stat. Mech. (2022) 093202.

[45] M. Biroli, H. Larralde, S. N. Majumdar, and G. Schehr, Phys. Rev. Lett. **130**, 207101 (2023)

[46] O. Vilk, M. Assaf, and B. Meerson, Phys. Rev. E **106**, 024117 (2022).

[47] S. Redner, *A Guide to First-Passage Processes* (Cambridge University Press, Cambridge, 2007).

[48] A. J. Bray, S. N. Majumdar, and G. Schehr, Adv. Phys. **62**, 225 (2013).

[49] S. N. Majumdar, Curr. Sci. **89**, 2076 (2005).

[50] https://github.com/MarcoBiroli/CriticalWalkers.